Structural Monitoring and Maintenance, *Vol. 4, No. 3 (2017) 195-220*
DOI: https:// doi.org/10.12989/smm.2017.4.3.195

A review on modelling and monitoring of railway ballast

Chayut Ngamkhanong[1,2a], Sakdirat Kaewunruen*[1,2] and Charalampos Baniotopoulos[1b]

[1]*Department of Civil Engineering, The University of Birmingham, U.K.*
[2]*Birmingham Centre for Railway Research and Education, The University of Birmingham, U.K.*

(Received August 26, 2017, Revised September 5, 2017, Accepted September 7, 2017)

Abstract. Nowadays, railway system plays a significant role in transportation, conveying cargo, passengers, minerals, grains, and so forth. Railway ballasted track is a conventional railway track as can be seen all over the world. Ballast, located underneath the sleepers, is the most important elements on ballasted track, which has many functions and requires routine maintenance. Ballast needs to be maintained frequently to prevent rail buckling, settlement, misalignment so that ballast has to be modelled accurately. Continuum model was introduced to model granular material and was extended in ballast. However, ballast is a heterogeneous material with highly nonlinear behaviour. Hence, ballast could not be modelled accurately in continuum model due to the discontinuities nature and material degradation of ballast. Discrete element modelling (DEM) is proposed as an alternative approach that provides insight into constitutive model, realistic particle, and contact algorithm between each particle. DEM has been studied in many recent decades. However, there are limitations due to the high computational time and memory consumption, which cause the lack of using in high range. This paper presents a review of recent ballast modelling with benefits and drawbacks. Ballast particles are illustrated either circular, circular crump, spherical, spherical crump, super-quadric, polygonal and polyhedral. Moreover, the gaps and limitations of previous studies are also summarized. The outcome of this study will help the understanding into different ballast modelling and particle. The insight information can be used to improve ballast modelling and monitoring for condition-based track maintenance.

Keywords: continuum model; finite element method, discrete element method; ballast; railway

1. Introduction

A traditional railway track (also called "ballasted track") consists of steel rails, sleepers located over ballast, sub-ballast and subgrade. This type of railway tracks is widely used all over the world for tram, metro, suburban and heavy haul rail networks. In general, ballasted track can be divided into two main components: superstructure and substructure. Superstructure, which is supported by substructure, comprises rails, fastening system, and sleepers and ballast. Substructure consists of ballast mat, sub-ballast and subgrade (Remennikov and Kaewunruen 2008).

The advantages of ballasted track are relatively low construction cost and use of indigenous

*Corresponding author, Ph.D., E-mail: s.kaewunruen@bham.ac.uk
[a] Ph.D. Candidate, E-mail: cxn649@student.bham.ac.uk
[b] Professor, E-mail: c.baniotopoulos@bham.ac.uk

http://www.techno-press.org/?journal=smm&subpage=7 ISSN: 2288-6605 (Print), 2288-6613 (Online)

material, ease of maintenance works, high hydraulic conductivity of track structure, good elasticity, and simplicity in design and construction. On the other hand, there are also some disadvantages of ballasted track such as degradation and fouling of ballast, requiring frequent track maintenance and routine check emission of dust from ballast resulting from high speed trains etc. Ballast is the significant component, which has several roles in ballasted railway track (Kaewunruen *et al.* 2014).

The functions of ballast are as follows (Selig and Waters 1994, Indraratna *et al.* 2011, Remennikov and Kaewunruen 2014 and Kaewunruen and Remennikov 2010):

- Transmit the load from sleeper/ballast interface to the sub-ballast and subgrade.
- Provide stability to the track by withstanding vertical, longitudinal, and lateral forces.
- Support sleepers uniformly.
- Provide adequate permeability for drainage and keep the sleepers in dry condition.
- Provide required degree of resiliency and degree of elasticity for track
- Absorb noise, vibration and energy

However, the most significant track deterioration is located on ballast. Ballast breakage can cause track deterioration and produce differential track settlement (Kaewunruen 2014). By nature, ballast has highly nonlinearities and heterogeneous due to the shape of ballast particle. Ballast particles, which are naturally sharp, angular, complex, and irregular, generally influence the track behavior so that ballast particle needs to be modelled accurately. To model this, continuum method has been considered for granular materials and extended to ballast. Mechanical behaviour of materials is modelled as a packed assembly of particles and continuous mass rather than as discrete particles.

The classical finite element method (FEM) can be used to solve this problem. Due to the discrete nature of ballast particles, it can be seen in many literatures that this approach could not perform the particle behaviour and difficult to highlight any significant phenomena. In reality, ballast breakage and track settlement caused by ballast become more significant. Ballast behaviour under moving train needs to be considered into individual particle. To consider discontinuities of ballast particles, discrete element method (DEM) is an approach that have been used for ballast and granular materials.

The infinite number of ballast in continuum approach is replaced by a finite number of ballast particles, which interact with its neighbours through the contact area. There are many types of particle shape, circular, spherical, super-quadric, and polyhedral, which have a different influence on the particle assembly (Hohner *et al.* 2013). It is important to note that ballast modelling is needed to model accurately because this element has a significant effect on track deterioration. The ballast degradation and deformation are not only influenced by particle shape but also gradation of ballast, amplitude and number of load cycles, confining pressure, ballast particle fracture strength etc.

This paper presents the approaches of ballast modelling divided into continuum method and discrete element method. A review of several analytical models employed in the ballasted track is also presented and explained. Moreover, the gaps and limitations are summarized and compared for better understanding in different case of study and suggestions for future work.

2. Ballast modelling

2.1 Continuum model

The continuum method has been widely used in many engineering problems over the time. In railway track, ballast has been replaced by continuum model, which is a homogeneous material and continuities. The finite element method (FEM) can be used to evaluate the result and solve the

problem of engineering. The finite element method has become widely used in railway track design. The ballast particles were considered as a continuum model by assuming ballast as infinitesimal size (Nguyen *et al.* 2003). Most of the literature, which considered the behaviour of ballasted track under passing train, used this approach for ballast modelling that can be modelled in many finite element software. These finite element commercial software available used for railway engineering, such as ILLITRACK, GEOTRACK, KENTRACK, TRACK2, ANSYS, LS-DYNA, ABAQUS, SAP2000, SIMPACK etc. The advantage of using continuum model as ballast is to reduce the computational time. Hence, this approach can be used in a whole track and very large structure, which requires more elements and computational time. However, the use of this approach cannot give some realistic behaviour and results especially in the local area such as dancing sleepers, initial settlement. Moreover, ballast particle shapes and distribution are not taken into account. Moreover, most traditional methods based on continuum model cannot simulate track fouling and settlement in a satisfactory manner. The interactions among ballast aggregate particles are mostly discontinuous.

There was a limitation in the literature for track settlement empirical models by Alve-Hurtado and Selig (1981), Shenton (1985), Sato (1995). Multi-axial stress strain properties in track substructure were not taken into account. A ballast block model was employed by Tutumluer (1995) as ballast to simulate the aggregate layer in pavement granular bases. The realistic properties obtained from direct shear test was used to model the particulate medium and found that the load transfer in granular materials was maintained by shear and normal compressive stresses at block interfaces since tensile stresses could not occur.

The tensionless nonlinear elastic model of 3D ballast was compared to the nonlinear elastic model in order to describe the tensional effect of granular material in continuum model (Nguyen *et al.* 2003). The vertical stresses in ballast were presented in both cases under quasi-static load. The result showed that the vertical stresses in the tensionless nonlinear elastic model were higher than those in nonlinear elastic model. It can be concluded from this study that the tensionless nonlinear elastic model weaker than that with tension. It is likely that the no-tension effect in granular structures is of great importance.

To accumulate degradation of settlement and subgrade of ballasted track, three-dimensional continuum models employing a constitutive relation of layered track substructure was applied. This model was first introduced for fine-grain granular materials (Sharp and Booker 1984, Abdelkrim *et al.* 2003 and Chazallon *et al.* 2012). This paper was applied this constitutive model to ballast. To measure long-term ballast settlement, the cyclic densification model (CDM) proposed by Suiker and Borst (2003) was used for continuum modelling. A three-dimensional finite element simulation using ABAQUS with linear-elastic subgrade material was employed. The influence of subgrade modelling was investigated and the result showed a large influence of subgrade model on ballast deformation.

To model substructure layers (Fig. 1): ballast, sub-ballast, soil mechanic and properties should be considered with the properties obtained from the experiment. A three-dimensional multilayer system modelled as a group of layers as explained by Esveld (2001), Sasaoka and Davis (2005), Ricci *et al.* (2005), Gallego *et al*. (2011) and Gallego *et al.* (2012), ballast, sub-ballast and subgrade, were simulated in a finite element 3D software to evaluate the behaviour of track under passing train. The results showed a great result in a whole track, which is one of the advantages of continuum model.

In case of the heavy-haul or high speed train, which can cause damage to the substructure or ballast breakage, nonlinearity of material should be considered appropriately. For the material's nonlinearity consideration, the Mohr-Coulomb plastic criteria was utilized during the numerical

simulation. However, some literatures suggested that the hardening soil model showed better agreement with the ballast strain hardening behaviour compared to the large scale tri-axial test considering ballast breakage (Indraratna *et al.* 2011). However, in ballast, this approach can show only the stress-strain distribution but cannot perform a detail in ballast particles, ballast breakage or local discontinuities. In addition, most traditional methods based on continuum analysis cannot simulate track fouling and settlement in a satisfactory manner. The interactions among ballast aggregate particles are mostly discontinuous. New modelling techniques need to be employed for studying ballast behaviour.

2.2 Discrete element method (DEM)

The Discrete element method (DEM) is an alternative method, which considers the nature of granular materials. This approach is a numerical method for computing the motion and effect of a large number of small particles with its interactions in a granular assembly. The discontinuous behaviour can be included. The discrete element method for granular material was first introduced by Cundall (1971) for rock and soil. Since railway ballast in the track generally comprises large particles of typical size approximately 40-60 mm, it is difficult to treat such a material as a continuum. However, DEM can provide insight into the micro-mechanical behaviour of railway ballast. Each ballast grain is represented as a rigid particle, which has an interaction and small overlaps with its neighbours. Moreover, ballast conditions, such as breakage (Lobo-Guerrero and Vallejo 2006, Lobo-Guerrero *et al.* 2006 and Mahmoud *et al.* 2016), settlement (Indraratna *et al.* 2005 and Thakur *et al.* 2009), densification and dilation (Indraratna *et al.* 2009 and Thakur *et al.* 2010), porosity (Wang *et al.* 2014), can be monitored using DEM.

3. Ballast particle shape

In general, ballast shape are naturally sharp, angular, complex, and irregular. There are several types of ballast shape that can be modelled for discrete element simulation.

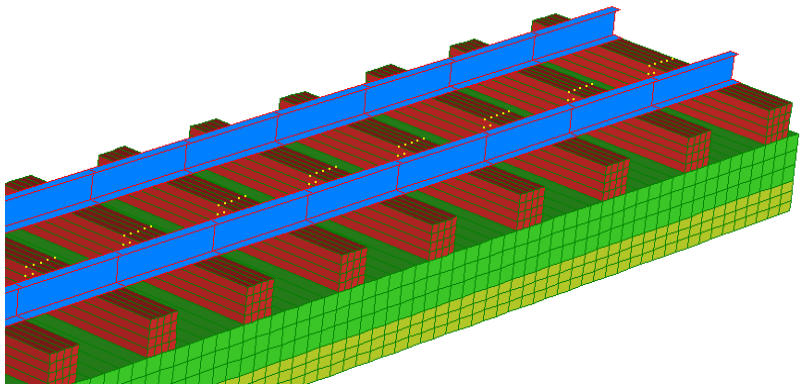

Fig. 1 Finite element mesh discretisation of ballasted track

(a) Circular (b) Circular cluster

Fig. 2 2-D particle shape

3.1 Circular and circular cluster

In the past, circular shape in 2-dimensional (Fig. 2(a)) was the first introduced shape for ballast particle modelling in which high-performance computer was not required. It should be noted that there are some limitations of simulating ballast as circular particles (Lobo-Guerrero and Vallejo 2006, Thakur *et al.* 2009 and Thakur *et al.* 2010). First, the obtained deformation was unrealistic because a weak interlock between each particle so that the deformation can be reduced considering angular particle. Hence, particle cluster (Fig. 2(b)) should be considered as angular particles to improve bond and ballast shape.

3.2 Spherical and spherical cluster

The 3-D model should be used instead of 2-D. In addition, the effect of ballast material lateral spread can be considered.

The 3-D spherical (Fig. 3(a)) elements have been widely used in recent years as can be seen in many studies (Matsushima *et al.* 2009, Garcia *et al.* 2009, Ferellec and McDowell 2010, Chen *et al.* 2014, Ngo *et al.* 2014, Yan *et al.* 2015, Xu *et al.* 2015 and Irazabel *et al.* 2017). This approach is more realistic than circular shape, which is a 2D shape. In order to create non-spherical or irregular shape, sphere cluster (Fig. 3(b)) have been used to generate more realistic shape than spherical shape. Sphere cluster consists of small spherical particles with overlapping. Generally, the appropriate number of spherical can be around 10-20 spheres as suggested by Indraratna *et al.* (2014). Spherical with different sizes can be adopted and mixed to improve ballast geometry. In addition, spherical cluster simulated by Kumara and Hayano (2016) using YADE has shown the closer stress-strain behaviour to the triaxial compression test than spherical. This approach is one of the ways and most popular to generate non-spherical particle. However, the use of angular or realistic particle in 3-D modelling would increase the number of particles and computational time.

(a) Spherical (b) Spherical cluster

Fig. 3 3-D particle shape

3.3 Super-quadric

Super-quadrics shape was defined by Barr (1981). This shape includes many shapes that resemble cubes, octahedra, cylinders, lozenges and spindles, with rounded or sharp corners. This shape has rarely been used as ballast shape because the shape of ballast is not similar to super-quadric and more difficult to create than spherical, which also requires less computational time. As can be seen in a previous study (Podlozhnyuk and Kloss 2015), the comparison of ballast particles between spherical and super-quadric showed that the computational time of super-quadric was 35 times higher than spherical.

3.4 Polygonal and polyhedral

In reality, ballast has a complex shape with sharp edge and corner so that polygonal for 2D and polyhedral for 3D (Fig. 4) are needed to model as ballast, which has more realistic than other shapes. However, this approach needs more computational time and high performance computer. In addition, more techniques are required in order to generate this shape. For example, Voronoi tessellation was used to create the randomly-shaped particle with the particle size of 37.5-50 mm (Elias 2013). The open source discrete element software YADE was employed. The volumetric stiffness was varied from $1.5x10^{11}$-$1.5x10^{13}$ while shear stiffness was equal to normal volumetric stiffness divided by 10^5. Contact normal force was calculated by least square fitting curve of a polyhedron surfaces intersection by tangent plane. Contact shear force was estimated by standard incremental algorithm. (Smilauer *et al.* 2010, Yade *et al.* 2010). The model was validated by oedometer experiment performed by Lim (2004) mechanics of railway ballast behaviour. However, ballast breakage was not considered in this study. Moreover, aggregate Imaging System (AIMS) and 3D digitization (3D scan) of real ballast grain surfaces provided by SNCF (Noura *et al.* 2016) can be also used to analyze the form, angularity, and texture of coarse aggregates and the angularity and form of fine aggregates. Nonetheless, polyhedral ballast has some limitation depending on elements and contact detection between polyhedrons, which lead to the limitation of particles. In addition, contact force determination on edges is also difficult and ambiguous (Lane *et al.* 2010). The advantages and disadvantages of each particle shape are summarized in Table 1.

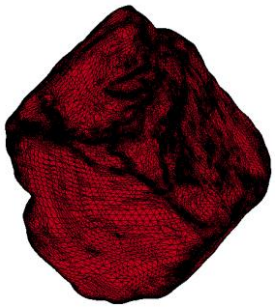

Fig. 4 Polyhedral ballast modelling

Table 1 Summary of advantages and disadvantages of different ballast particle shape

	Circular	**Circular cluster**	**Spherical**	**Spherical cluster**	**Polygonal and Polyhedral**
Dimensional	2D	2D	3D	3D	2D, 3D
Shape	Regular (Simplified shape), Unrealistic	Irregular (better for overlapping circular cluster), Realistic	Regular, Unrealistic	Irregular (better for overlapping spherical cluster), Realistic	Irregular (match real particle shape), Realistic
Contact interlocking	Weak	Strong	Weak	Strong	Strong
Computational time	Medium	high	high	high	highest
Limitation	2D, Ballast behaviour is unrealistic	Many circulars of various size are required	Particle behaviour is unrealistic	Many spherical of various size are required	Contact detections are difficult to define

4. Contact detection

4.1 Contact detection for circular and spherical

The overall constitutive behaviour of a material is simulated in PFC^{3D} (Itasca 2003) by associating a simple constitutive model with each contact. The constitutive model acting at a particular contact consists of three parts:

- A stiffness model (consisting of a linear or a simplified Hertz-Mindlin Law contact model)
- A slip model, and
- A bonding model (consisting of a contact bond and/or a parallel bond model).

4.1.1 Contact stiffness model

The contact stiffness model comprises the contact force, shear and normal, with respect to relative displacement. The contact stiffness model can be classified into two types: linear model and Hertz-Mindlin model.

Linear model

In reality, the ballast support is made of loose, coarse, granular materials with high internal friction. It is often a mix of crushed stone, gravel, and crushed gravel through a specific particle size distribution. It should be noted that the ballast provides resistance to compression only.

A linear elastic model was first introduced by (Cundall and Strack 1979) in order to simulate the contact between granular materials in two-dimensional. This contact model has been widely used to

simulate aggregate interactions (Abbas *et al.* 2007). The normal stiffness is a secant stiffness, which related to the increment of normal force to the normal displacement. Whilst the shear stiffness is a tangent stiffness, which related to the increment of shear force linearly to the shear displacement.

The contact-stiffness model can be computed as shown in Eqs. (1) and (2).

$$K^n = \frac{K_n^A K_n^B}{K_n^A + K_n^B} \tag{1}$$

$$K^s = \frac{K_s^A K_s^B}{K_s^A + K_s^B} \tag{2}$$

Where K_n^A and K_n^B are the normal stiffness of object A and B
K_s^A and K_s^B are the shear stiffness of object A and B

Hertz-Mindlin model

For normal contact, the theory of frictional elasticity of sphere was first introduced by Hertz (1882) called Hertz model. The Hertz model provides a nonlinear solution for normal contact whilst the nonslip model developed by Mindlin and Deresiewicz (1953) was then used for tangential direction. Hertz theory, which is more complicated than linear model, has been used to consider the shape of spherical (Mindlin and Deresiewicz 1953). Due to the complexity of conventional approach, the Hertz-Mindlin developed by Mindlin and Deresiewicz (1953) have been used to replace the original. This model is defined by the elastic properties of two spherical as shown in Fig. 5. It should be noted that tensile force is not defined and the contact force increase together with the increase of overlap in Hertz-Mindlin model. The resulting force for Hertz-Mindlin can be calculated as shown in Eqs. (3)-(5).

Hertzian pressure relationship can be seen

$$P(r) = p_0(1-(\frac{r}{a})^2)^{1/2} \tag{3}$$

Where $p_0 = \left(\frac{3P}{2\pi a^2}\right)$ and $a = \left(\frac{3PR^*}{4E^*}\right)^{1/3}$

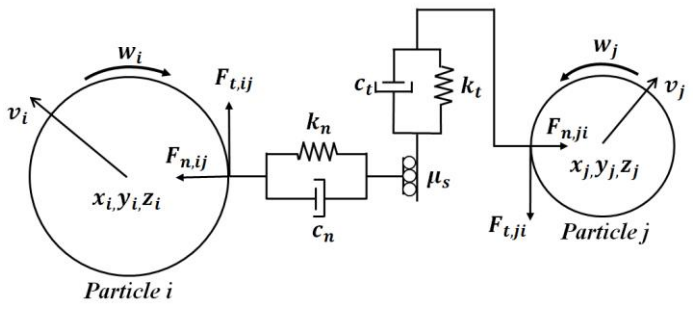

Fig. 5 Hertz-Mindlin model (Chung and Ooi 2008)

Then, the resulting elastic force $\boldsymbol{F_n^E}$ can be computed by replacing P

$$F_n^E = -\frac{4}{3}(E^*\sqrt{R^*}U_n^{0.5})U_n \tag{4}$$

Where $R^* = \frac{R_A R_B}{R_A + R_B}$ and $1/E^* = \frac{1-\nu_A^2}{E_A} + \frac{1-\nu_B^2}{E_B}$

E is the equivalent young modulus, $R^*$is the equivalent radius of object A and B

While the resulting shear force $\boldsymbol{F_t}$ can be calculated as follows

$$F_t = -\frac{2}{8}(8G^*\sqrt{R^*}U_n^{0.5})U_t \tag{5}$$

Where G is the equivalent shear modulus

However, the comparison between linear model and Hertz-Mindlin model was proposed by Di Renzo and Maio (2005). The results showed that linear model gave a better result than Hertz-Mindlin model when the parameters of the linear model were precisely evaluated. Nonetheless, Hertz-Mindlin should be used when spherical shapes are considered and to perform motion deeply on granular material.

4.1.2 Slip model

The slip model acts between broken contact bonding of two spherical or unbonded objects. The maximum can be computed as follows

$$F_{\max}^s = \mu\left|F_i^n\right| \tag{6}$$

Where F_{max}^s is the allowable shear contact force, μ is the friction coefficient at the contact (smaller value of the two contacting entities), and F_i^n is the normal component of contact force

Slip occurs when $\left|F_i^n\right| > F_{\max}^s$

4.1.3 Bonding model

In the spherical bonding, there are two bonding models: a) contact bond model and b) parallel bond model.

Parallel bond model

The parallel bond (Fig. 6(a)) can transmit normal force, shear force, and bending moment between the spherical. The force and moment death with parallel bond can be denoted into normal and shear components by F_n, F_s, M_n, and M_s. The parallel bond breaks when stress occurred exceed the parallel bond strength. The maximum normal and shear stress at the bond perimeter can be computed as shown in Eqs. (7) and (8).

$$\sigma_{\max} = \frac{\left|F_n\right|}{A} + \frac{\left|M_s\right|}{I}R \tag{7}$$

$$\tau_{\max} = \frac{|F_s|}{A} + \frac{|M_n|}{J} R \tag{8}$$

Where R is the radius of bonding disk defined as spherical radius, A is the area of bonding disk, I is the moment inertia of bonding disk, and J is the polar moment of bonding disk.

Contact bond model

The contact bond (Fig. 6(b)) can only transmit normal force and shear force. There is no resistance to rolling of a spherical bond because this contact bond acts over a vanishingly small contact area without bonding disk. The contact bond breaks when stress occurred exceed the tensile strength or shear strength.

4.2 Contact detection for polygonal and polyhedral

The contact algorithm between non-spherical is very complicated compared to the sphere contact. For non-spherical, a special approach contact detection algorithm of contact force has to be developed. It was observed that about 80% of computational time are taken by contact detection between particles. For polygonal (2-D) and polyhedral (3-D) particles, Particles are assumed to be convex, rigid or deformable, while concave particles can be modelled as a combination of several convex particles attached to each other. The common plane (CP) was introduced by Cundall (1988) to bisect two contacting particles. There are three approaches to obtain common plane: common plane method, fast common plane method (FCP) and shortest link method (SLM).

4.2.1 Common plane method or inner potential approach (Contact between polyhedron)

To evaluate contact force between polyhedrons, Common Plane (CP) method developed by Cundall (1988) is the first approach to bisect the space between two particles by common plane. Two particles intersect the CP when both are in contact. On the other hand, neither intersects the CP when both are not in contact. An approach to obtaining the CP for polygonal (2-D) and polyhedral (3-D) particles are as follows.

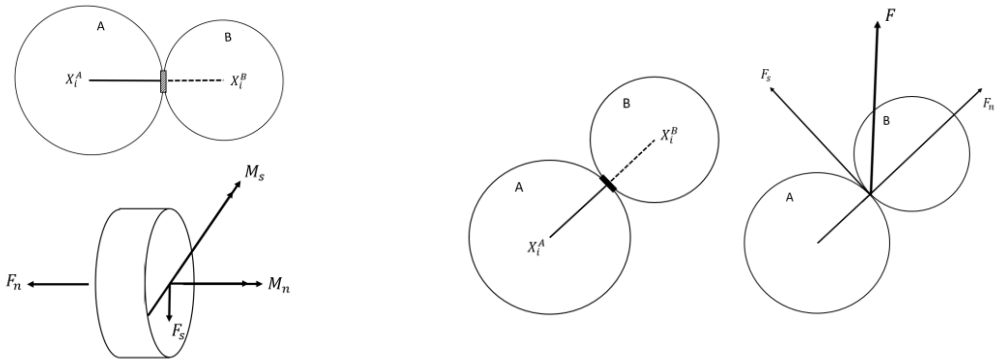

(a) Parallel bond model (b) Contact bond model

Fig. 6 Bonding model

The 'distance' dV of any point V in the space to any arbitrary plane is defined as in Eq. (9)

$$d^V = n \cdot (V_0 - V) \tag{9}$$

Where n is the unit vector normal to the plane and V0 is any point on the plane

For two particles A and B, the distance from CP to the nearest vertex can be defined as in Eqs. (10) and (11).

$$d_B = \min \left\{ n_i V_i^{(B)} \right\} \tag{10}$$

$$d_A = \min \left\{ n_i V_i^{(A)} \right\} \tag{11}$$

Where d_A is the distance to the nearest vertex on A

d_B is the distance to the nearest vertex on B

$V_i^{(A)}$ is the position vector of a vertex on A

$V_i^{(B)}$ is the position vector of a vertex on B

For any two particles A and B, a CP is a plane that satisfies the following three conditions:

- Centroids of particles A and B are located on opposite sides of the CP. It is assumed that particle A is the one with its centroid in the left side (negative) and B is the one with its centroid in the right side (positive) of CP as can be seen in Fig. 7.
- The gap between two particles can be defines as $d_B - d_A$
- $d_A = -d_B$

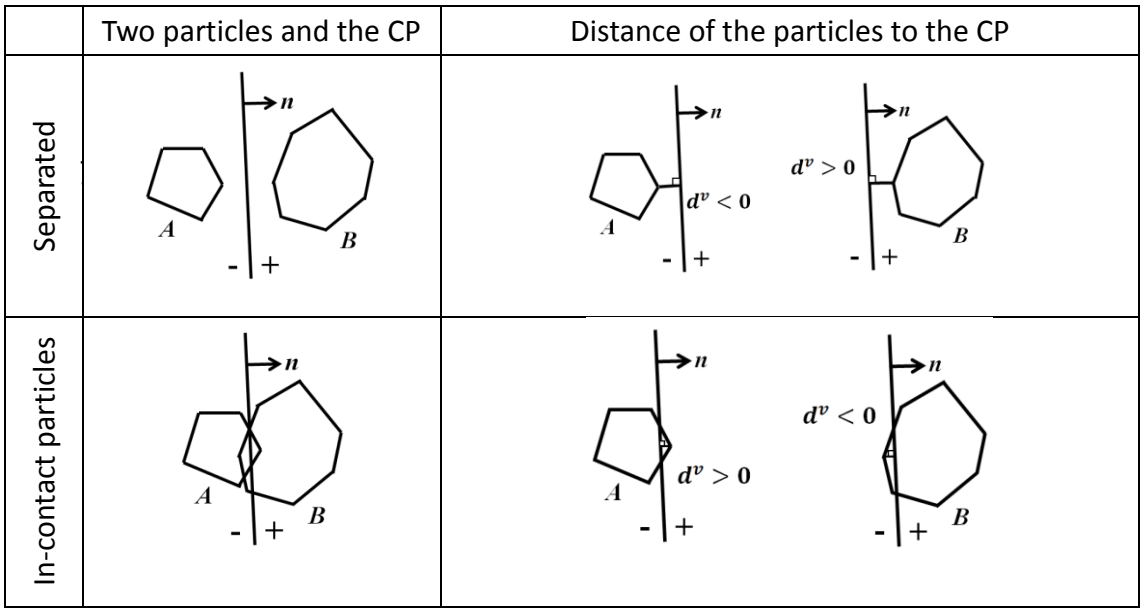

Fig. 7 The CP and its distance to the particles (Nezami *et al.* 2004)

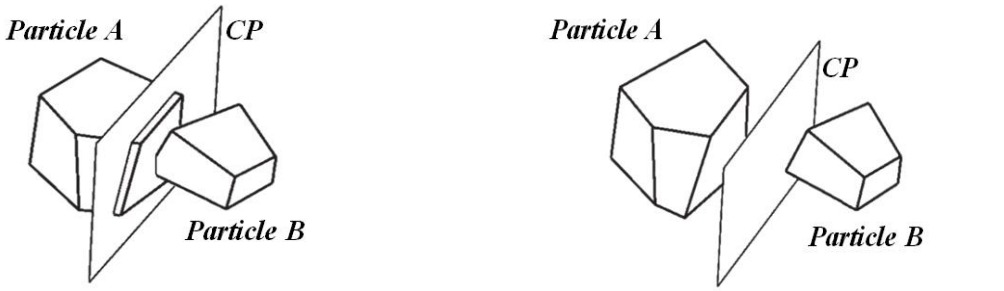

(a) particles in contact, both particles intersect the CP

(b) particles not in contact, neither particle intersects the CP

Fig. 8 Common plane (CP) between two particles (Nezami *et al.* 2006)

Fig. 8 shows the location of CP and particles. Particle A and B are located on negative and positive side, respectively, which means that when $d_A < 0$ and $d_B > 0$, the particles are not in contact or there is a gap between two particles. On the other hand, the particles are in contact when $d_A > 0$ and $d_B < 0$.

An iterative process of finding common plane (CP) proposed by Cundall (1988) involve translation and rotation of CP. The total number of iterations is normally large especially on the first step depending on the accuracy of the initial guess of the CP.

4.2.2 Fast common plane (FCP)

The fast common plane was then proposed by Nezami (2006) for identifying the CP. The number of candidate CP can be reduced to 5 candidate planes. Hence, the computational cost and iteration processes can also be reduced significantly. The common plane identification can be concluded as follows (Nezami 2004):

- CP should pass through the midpoint M of segment AB.
- CP is completely located within the space S (If the perpendicular bisector is located within the space S, PB is the common plane. On the other hand, the common plane is the line with the smallest angle to the PB when PB is not located inside the space S).
- Where the space S is the area formed by *Mm1, Mm2, Mm3 and Mm4* as can be seen in Fig. 10
- CP should produce the smallest angle with the perpendicular bisector (PB) of the line AB.
- CP is one of the five candidate planes.

4.2.3 Shortest link method (SLM)

For any two particles, which are not in contact, shortest link method is used as an alternative approach to find the common plane. In case of particles in contact, SLM shows the same scheme as FCP.

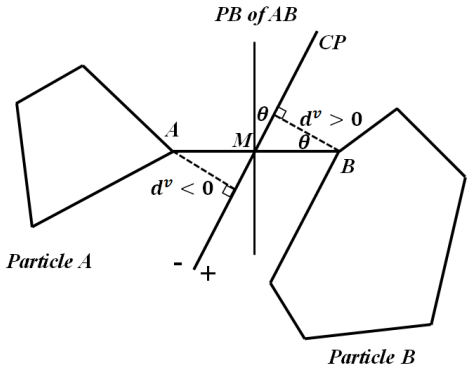

Fig. 9 Perpendicular bisector (PB) of AB (Nezami *et al.* 2004)

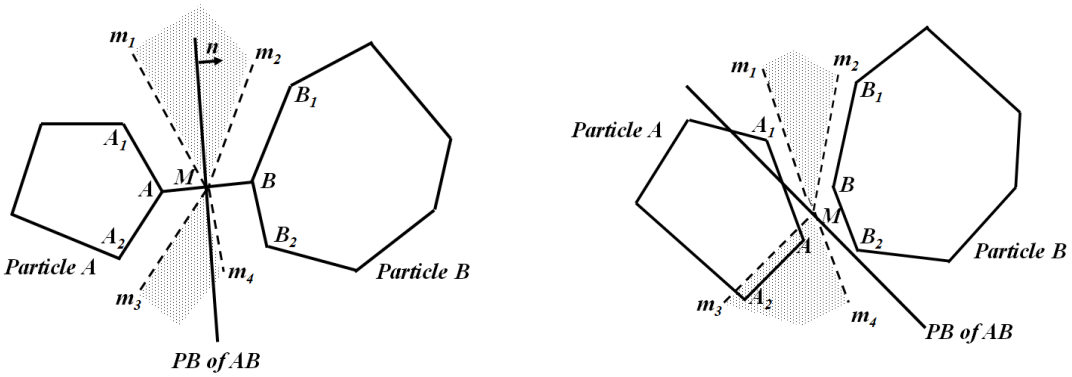

(a) Inside space S, PB is CP (b) Outside space S, line Mm_1 is CP

Fig. 10 Perpendicular bisector (PB) of AB and the common plane (CP) (Nezami *et al.* 2004)

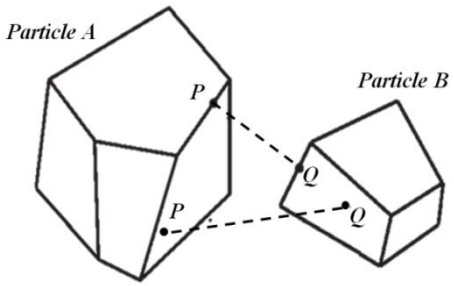

Fig. 11 A link between P on surface of particle A and Q on surface of particle B (Nezami *et al.* 2006)

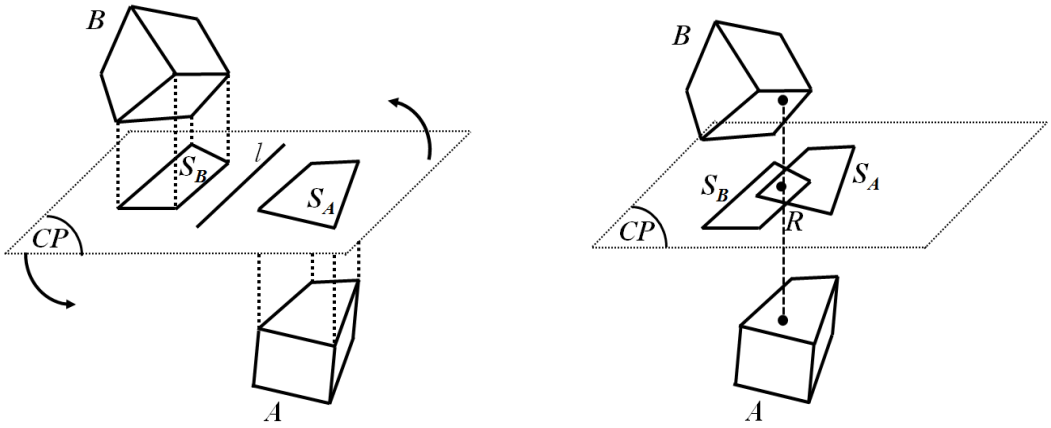

(a) $S_A \cap S_B = \varnothing$ (b) $R \in S_A \cap S_B$

Fig. 12 Projection of closest points on the CP (Nezami *et al*. 2006)

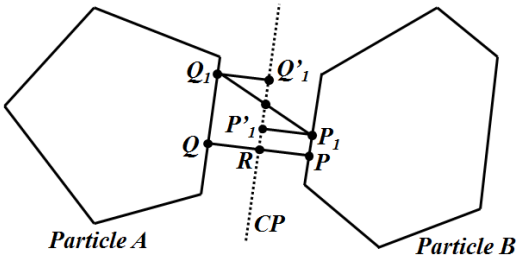

Fig. 13 PQ is the shortest link between the two particles (Nezami *et al.* 2006)

PQ is the link between two particles that connects point P on the surface of Particle A to point Q on the surface of particle B, as shown in Fig. 11. The perpendicular bisector plane (PCB) of the shortest link between two particles is the CP. The projections of the closest point on the CP from the particles consist of two projection plane, S_A and S_B as shown in Fig. 12. If both planes are not in contact or no overlap then the CP is needed to rotate about l until the S_A and S_B have at least one point in contact. It can be seen that the gap between two particles is larger.

Fig. 13 shows the link (PQ and P_1Q_1) between the two particles. P_1Q_1 is an arbitrary link, R is the point of intersection on CP and P_1' and Q_1' are the projection points of P_1 and Q_1 on CP. It can be seen that

$$\left|P_1Q_1\right| = \left|P_1R_1\right| + \left|Q_1R_1\right| \geq \left|P_1P_1'\right| + \left|Q_1Q_1'\right| \geq \left|PR\right| + \left|QR\right| = \left|PQ\right| \tag{12}$$

or

$$\left|P_1Q_1\right| \geq \left|PQ\right| \tag{13}$$

Hence, PQ is the shortest link between two particles and CP is the perpendicular bisector plane for PQ.

Three approaches (common plane method, fast common plane method and shortest link method) were compared for both 2D and 3D models. The BLOCKS3D version 2.0 developed by Nezami *et al.* (2004) was used for 3-D polyhedral. The 3-D polyhedral were simulated by dropping the particles into a cubic box until the final stable. The speed up ratio computed by the ratio of the CPU run time spent in CPU detection subroutine between CP method and FCP or SLM. The results showed that the speed up ratio decreased with an increasing number of particles. It was observed that the speed up ratio are 12 and 18 for FCP and SLM.

5. Ballast breakage, densification and dilation

In reality, the ballast track degradation under the cyclic loading by train induces settlement of ballast layer. The degradation is one of the most criteria in designing ballast particle size distribution that enhance track durability. As can be seen in previous studies, there are two main approaches to comprehend the mechanism of ballast breakage. Firstly, the experiment, such as uniaxial test, bi-axial, oedometer etc., can be conducted in laboratory. Another method is to use discrete element method to simulate ballast behaviour and rupture. In the beginning, discrete element method implementations cannot consider crushing of ballast. Due to the computational time, most recent decades did not consider particle crushing to occur.

To simulate ballast breakage in DEM, two different solutions have been studied. The first method is to model each particle as a cluster of bond particles. The load can break the bond, which holds the particles together.

Another method of ballast breakage simulation is to replace the original geometry with an equivalent group of smaller particles.

The loading on particle can be seen in Fig. 14(a) where induced stress can be calculated by the maximum contact force acting on particle as shown in Fig. 14(b), where L is the thickness of disk and D is the diameter of disk. The produced fragments after failure were presented by Lobo-Guerrero and Vallejo (2006), Mahmoud *et al.* (2016), Lobo-Guerrero *et al.* (2006).

As can be seen in Fig. 14(c), the particle was divided into 8 fragments. There are three different sizes (0.5D, 0.33D and 0.167D). Only these fragments can replace the broken sleeper.

Ballast breakage index was presented by Indraratna *et al.* (1998). This index can be calculated from fraction passing-sieve size relationship as can be seen in Fig. 15. A is the area between initial PSD and final PSD while B is the area between final PSD and arbitrary boundary of maximum breakage due to ballast degradation. Ballast breakage index can be calculated in Eq. (14).

$$BBI = \frac{A}{A+B} \tag{14}$$

After loading, it can be seen that ballast particles size became smaller, which can cause a shift in the distribution curve without the change in the largest particles. The boundary of maximum breakage was assumed to be linear from the minimum sieve size (2.36 mm) to d-95 of the maximum sieve size.

The degradation of coarse aggregates under static loading provides an important insight into degradation under cyclic loading. This is because the particle breakage taking place under static loading can be considered as the preliminary modelling step of repeated loading. The extent of

particle breakage during the first stage of cyclic loading is expected to be relatively high.

To consider cyclic loading, the previous studies of static loading can be used as a preliminary behaviour in the first step of cyclic loading. The cyclic loading was then studied after static loading to consider ballast degradation with more load cycles. The 500 cycles-harmonic loading was applied by a dynamic actuator with the frequency of 20 Hz. Deviator stress used were 230, 500, 750kPa. Ballast breakage index was computed with varying confining pressures and static loadings. The different confining pressure can be divided into 3 parts with respect to bond breakage as previously presented by Indraratna *et al.* (2005).

- Dilatant, unstable degradation zone (DUDZ), this zone showed a significant increased trend in bond breakage when confining pressure was reduced. This is because the poor contact between each particle.
- Optimum degradation zone (ODZ), this is the optimum value of confining pressure, which can reduce ballast breakage because of the optimum particle configuration and internal contact stress distribution.
- Compressive, stable degradation zone (CSDZ), within this zone of confining pressure, the bond breakage showed a slight upward trend when confining pressure was risen because of an increase in stress at contact and restriction of internal particle movement.

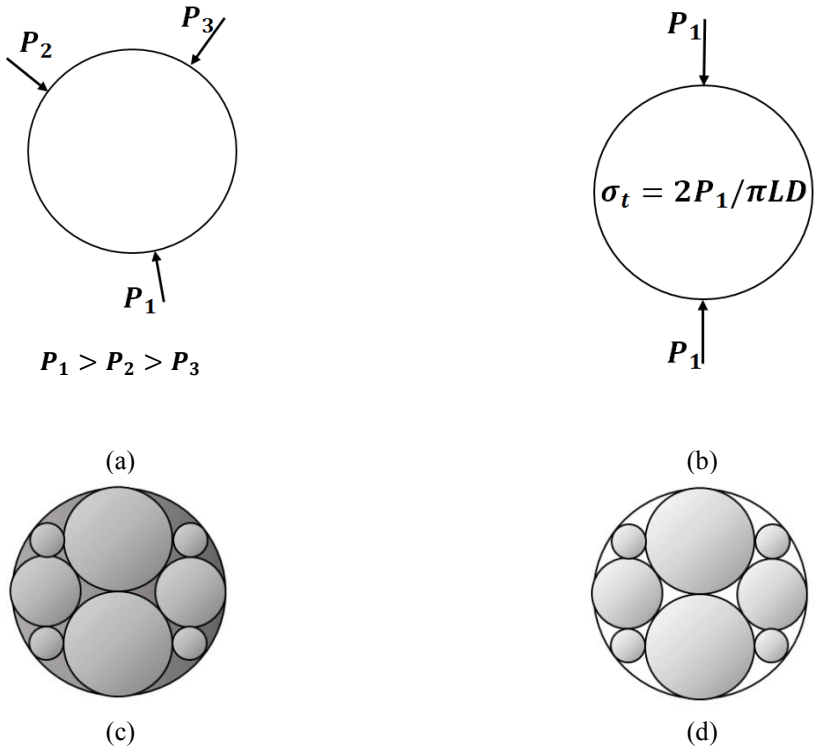

Fig. 14 Idealization of the induced tensile stress and the produced fragment after failure (Lobo-Guerrero and Vallejo 2006)

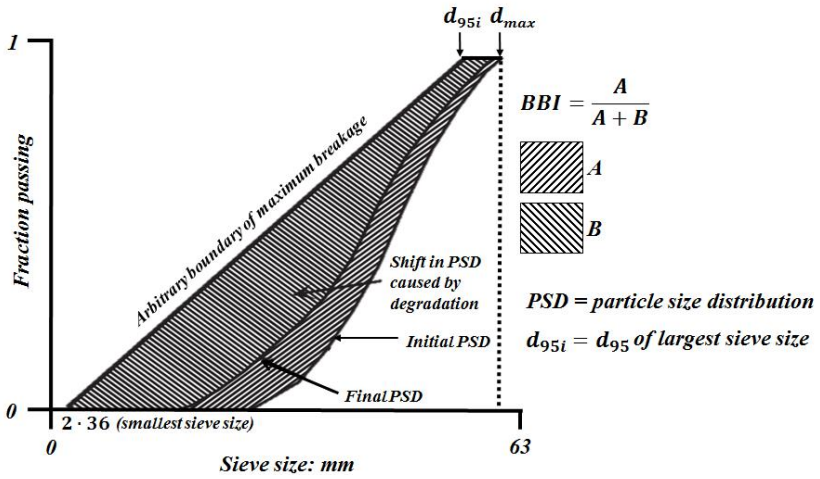

Fig. 15 Simplified breakage index for ballast degradation (Indraratna *et al.* 1998)

Effect of confining pressure

The ballast breakage considering confining pressure has been studied in many researches. Static loading has been applied as can be seen in recent studies (Marsal 1973, Indraratna *et al.* 1993, Indraratna *et al.* 1998 and Indraratna and Salim 2002).

The benefits of confining pressure are to prevent various problems such as ballast breakage, track buckling, spreading of ballast. In addition, the decrease of dilatancy can be observed at high confining pressures (Zhou *et al.* 2016). On the other hand, dilatancy can be increased at low confining pressures due to the increase of intermediate principal stress ratio.

The confining pressure provided by ballast shoulder and sleepers were generally in the range from 5-40kPa (Selig and Alva-Hurtado 1982), which is very small compared with vertical loading. From the tri-axial static testing conducted in laboratory, rate of ballast breakage can be increased when confining pressure was increased in the compressive, stable degradation zone. Ballast degradation can be observed with broken ballast. These particles became smaller and less angular, which can lead to the decreasing of shear strength.

Nonetheless, the effect of cyclic should be taken into account instead of static loading because the trains run frequently and induce more settlement of ballast. Discrete element modelling of ballast under cyclic biaxial tests considering ballast particle breakage were proposed by Thakur *et al.* (2009). In this study, ballast particle size (rectangular, circular and triangular) were varied from 19 to 53 mm. Standard Australia (1996) was considered as ballast gradation. AUTOCAD were used to generate ballast shape and small tangential circulars were filled on another layer. Parallel bond was installed between each particle in order to make ballast breakage. The 1000-loading cycles, which corresponding to 150 km/hr train velocity on standard gauge track in Australia was applied. Confining pressure was varied from 10 to 240KPa. The results demonstrated that ballast particle with low confining pressure had a higher axial strain and bond breakage. In case of high confining pressure, the permanent deformation was stable even if ballast particles degraded. This was because

the effect of confining pressure. In addition, the permanent deformation of ballast and particle breakage increased with the frequency and number of load cycles. The results were then compared to previous experiment conducted by Indraratna *et al.* (2005), as shown in Fig. 16. It is clearly seen that the DEM result followed the same trend as experiment done by Indraratna *et al.* (2005). It can be concluded that the number of load cycle also play a role on the ballast settlement and densification.

From the literature, it can be concluded that the highest ballast breakage index occurs when the confining pressure is lower than 10KPa. The optimum value of confining pressure should be in optimum degradation zone (ODZ) as smallest the number of ballast breakage occur. As a consequent, confining pressure between 30-75KPa can prevent ballast breakage and also other problems.

The comparison between ballast with and without breakage was also studied by Lobo-Guerrero and Vallejo (2006). Discrete element method using PFC2D and FISH language developed by Lobo-Guerrero and Vallejo (2006) was used to model and study ballast degradation subjected to 200 load cycles. The 2-cm circular ballast particles were placed randomly in the box, which had a shear stiffness of $1x10^9$ N/m and friction coefficient of 0.7. The normal, shear stiffness and friction coefficient were set to $1x10^8$ N/m, $1x10^8$ N/m, and 0.7, respectively. This simulation was comprised of three sleepers over the ballast bed. The sleepers were moved downward with the velocity of $5x10^{-7}$ m/step until the contact force equal to 62 kN. The permanent deformation of ballast in the crushable case was higher than uncrushable case even if there were only a few broken particles. Moreover, it was observed that ballast breakage mostly occurred underneath the sleepers during the first load cycle. However, it should be noted that the actual deformation should be reduced due to poor interlocking between each circular particles.

The ballast cracking begins when bond breakage and particle will split into small particles with weakening contact force**.** The irregular ballast particles are constructed randomly from 37 mm to 51 mm. SDEM code (Sphere-based discrete element method) developed by Yan *et al.* (2015) was used to generate spherical cluster with 5 mm diameter of sub-sphere**.** Each particle was connected by parallel bond to prevent the relative rolling between sub-spheres. The result showed that more spherical the particles are, the higher the breakage strength is and the stress required to break a small particle may be rather higher than larger particles.

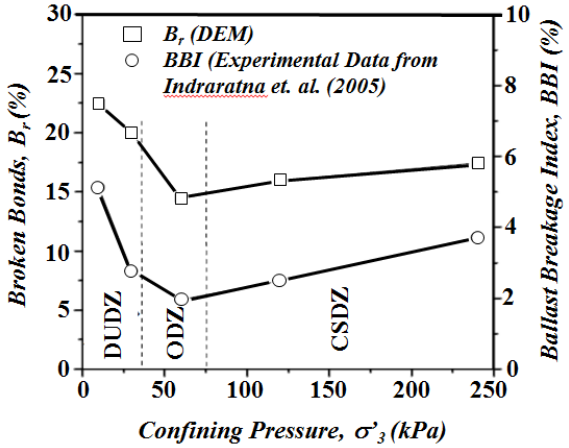

Fig. 16 Particle breakage at various σ'_3 and comparison of breakage trends observed in the DEM with the experiment (Thakur *et al.* 2009)

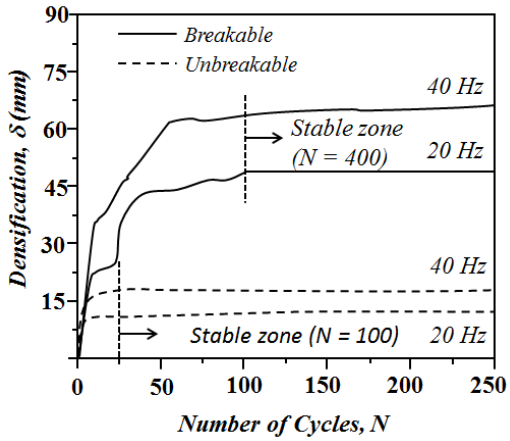

Fig. 17 Comparison of cyclic densification (breakable and unbreakable particles) (Thakur *et al.* 2010)

For capturing stone angularity in DEM modelling, software code PFC^{2D} were used. There were two approaches to represent ballast shape (Mahmoud *et al.* 2016). Firstly, 2-D small circular elements were assembled with inner particle bond to represent hexagonal closed-packed. MATLAB was used. Another approach was represented by continuing first approach by filling each with tangential circular elements using AutoCAD. The advantage was to minimize the number of elements and computation time (use the same method as Thakur *et al.* 2009). However, PFC^{2D} has a limitation on shape modelling, which can handle only circular shape so that irregular ballast need to be modelled by assembling of circular elements. Aggregate Imaging System (AIMS) database obtained 2D images of ballast particles. Simplified method was also used to compare the results with the two approaches presented. Single circular particle were represented as ballast particles using the parameters from Lobo-Guerrero *et al.* (2006) and Lobo-Guerrero and Vallejo (2006). Ballast particles were placed randomly without overlap between the particles. The velocity of $1x10^{-7}$ m/step was set as sleeper velocity in downward direction until the contact force is equal to 62kN, which was suggested by Lobo-Guerrero *et al.* (2006) and Lobo-Guerrero and Vallejo (2006). The 200 loading cycles with varying contact bond strength were conducted. The results showed that the simplified method had some disadvantages. For example, the ballast shapes were not realistic and the crushing locations were located only underneath sleepers, which are different from first two approaches. The first approach illustrated more realistic result than the second method especially when ballast breakage occurred because there were the large ballast particles remaining in the second approach.

The cyclic biaxial testing of ballast with the confining pressure of 60MPa was conducted to measure ballast breakage and densification using 2-D circular cluster (Thakur *et al.* 2010). The frequencies of 20 and 40 Hz were applied with the 1000 cycles of load consisting of unbreakable and unbreakable particles. The results show the influence of ballast breakage and the number of load cycles on ballast densification as can be seen in Figs. 17 and 18. The densification of unbreakable ballast was reached the stable zone at 100 cycles whilst the 400 cycles were observed in case of breakable ballast. In addition, the maximum unbreakable ballast densifications were around 12 and 17 mm at 20 Hz and 40 Hz, respectively whereas for breakable particles, 45 mm and 67 mm were observed at 20 Hz and 40 Hz, respectively.

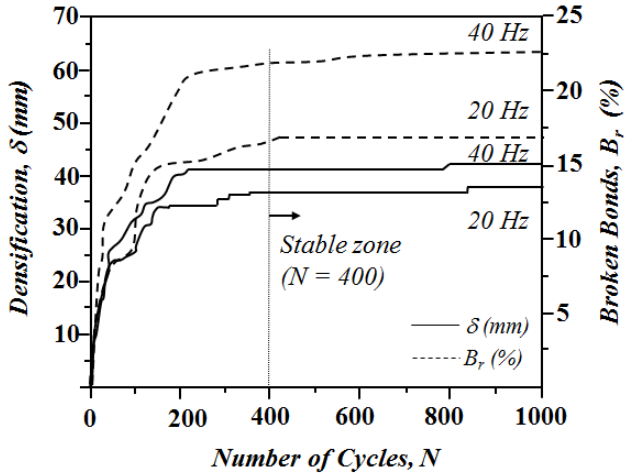

Fig. 18 Effect of bond breakage on cyclic densification (Indraratna *et al.* 2009)

The cyclic loading on sleeper over the discrete ballast model has been studied as can be seen previously. In realistic, the train may generate not only static, quasi-static load but also impact load. Most of the previous studies focused on the static and cyclic loading, which were unrealistic, the dynamic cyclic loading due to passing train and wheel rail irregularities should be considered in future work because this load may cause higher permanent deformation and breakage of ballast. There were few studies focused on impact load on sleeper with the discrete element modelling of ballast.

Transient response analysis was performed by Aikawa (2017) to countermeasure the ballast settlement using high-damping under sleeper pad. Advance/FrontSTR software was used. The discrete element method was used together with finite element method in order to construct tetrahedron ballast particle. All particles consisted of small finite solid element model. Each discrete particle was divided into one thousand finite elements. The 56 rectangular ballast blocks were assembled to perform the full scale size of ballast under sleeper. The contact between ballasts and sleeper was modelled as nonlinear contact spring with tensionless contact because the jumping motion of ballasted track was observed from the experiments. However, the discrete element modelling of ballast during the passing train has not been studied and considered. In further study, these should be taken into account to validate the results from previous studies.

From the previous studies, the comparison between continuum model and discrete element model can be summarized in Table 2. In summary, the multi-layer continuum model using finite element method can be used to evaluate the substructure, whole track behaviour and train-track interaction Esveld (2001), Ricci *et al.* (2005), Sasaoka and Davis (2005), Gallego *et al*. (2011) and Gallego *et al.* (2012). However, ballast discontinuity and deterioration such as ballast breakage are not taken into account, which leads to the lack of modelling. The discrete element model is an alternative approach with more benefits and covers more details and ballast condition, which could not be considered in continuum model, such as ballast discontinuity, particle interaction, ballast fouling, ballast breakage etc. (Indraratna *et al.* 1998, Lobo-Guerrero and Vallejo 2006, Lobo-Guerrero *et al.*

2006, Mahmoud *et.al.* 2016 etc.). Nonetheless, this approach requires higher computational time and memory consumption due to the large number of particles and contact algorithms Cundall (1988), Xu *et al.* (2015) and Irazabel *et al.* (2017). The whole track behaviour and train-track modelling have not been investigated in recent studies. The ability of ballast and track support materials to suppress broadband vibrations (e.g. using ballast as a meta-material) has not well been reported (Kaewunruen and Kimani 2017, Kimani and Kaewunruen 2017). Only the testing simulations have been studied to validate the results from the experiment conducted in laboratory (Thakur *et al.* 2009, Thakur *et al*. 2010).

Ballast deteriorations (breakage, settlement, densification and dilation) are the main problem of track deteriorations that the routine maintenances are required. The maintenance of track sections with severe levels of ballast deterioration must take priority over all other maintenance in the railway network (Prescott and Andrews 2013, Setsobhonkul *et al*. 2017). Ballast condition should be monitored in order to avoid high level of deterioration and enable predictive, condition-based track maintenance. As can be seen in the open literature, DEM simulation can help computing ballast breakage and settlement under repeated load corresponding to moving train. The method can also enable the estimation and optimal redesign of ballast as meta-material (BAM) at critical locations (Kaewunruen and Mirza 2017). Ballast maintenance, such as tamping, stabilizing, regulating, and ballast renewal, is the method to squeeze or compact the ballast beneath the sleeper and maintain the track alignment. This method is frequently used when the high settlement and void beneath sleeper are observed. It is possible to accurately estimate track behaviour using DEM approach because the insight into particles interaction can help track inspection. The ballast fouling and contamination, and drainage capacity could also be estimated. DEM simulation is likely to improve the track inspection and predictive maintenance thinking/planning even if the whole train-track behaviour using DEM have not been investigated.

Table 2 Comparison between continuum model and discrete element model

	Continuum model	Discrete element model
Method	FEM	DEM, DEM-FEM
Ballast discontinuity	×	✓
Particle interaction	×	✓
Ballast fouling	×	✓
Ballast breakage	×	✓
Whole track behaviour	✓	×
Train-track modelling	✓	×
Computational time	Low	High
Memory consumption	Low	High

6. Conclusions

The conventional track (also called "ballasted track") has been widely used throughout the world. Ballast is the main components, which transmit the load from sleeper/ballast interface to the sub-ballast and subgrade. Due to the increase of higher speed and demand of railway transportation, the ballast and substructure can be experienced large deformation and deterioration. Ballast degradation, fouling and breakage are the main causes, which can lead to track settlement and degradation. In particular, recent studies have been conducted ballast modelling using continuum model. The finite element method (FEM) is often used for constitutive model of a multilayer substructure: ballast, sub-ballast, and subgrade. The advantages of using continuum model are to reduce the computational time and memory consumption, which can lead to the use of analysing of large-scale ballasted track under the passing train. On the other hand, the results obtained from FEM are difficult to handle the discontinuous behaviour and material nonlinearities of ballast. The FEM can only demonstrate the stress strain distribution without specific location of particle breakage, fouling and damage occurred. Therefore, the new modelling technique called discrete element method (DEM) has become an alternative method that provides a discontinuous behaviour, particle size distribution, connection between each ballast particle etc. The 2-D circular shape was first introduced in granular material with a limitation of interlocking between each particle. In 3-D, spherical and spherical cluster consisted of small spherical have been used in order to create an irregular shape. Another shape is polyhedron, which provides a realistic shape of ballast. The polyhedral ballast is constructed by both finite element method (FEM) and discrete element method (DEM). The discrete polyhedral, which has individual finite element mesh, are constructed together with contacting between each particle. The difficult part is to model an irregular shape so that the Voronoi tessellation and aggregate Imaging System (AIMS) are needed. However, the higher computational time and memory consumption are required to generate discrete particle. Hence, recent studies have conducted the ballast modelling under only static and cyclic load. Only a few studies have studied the impact response of ballast. The field measurements and experiments, such as oedeometer, biaxial, triaxial, were then used to validate all the results from the theoretical model. For ballasted track, it can be seen from the literature that the discrete element of ballast under passing train have not been fully investigated. Only one bay ballasted track with sleepers have been considered under transient load corresponding to train load. However, the insight into the ballast behaviour using discrete element modelling will help ballast inspection and predictive maintenance of ballast and track. The outcome of this study will not only improve the better understanding into ballast behaviour and modelling under different conditions and limitations but also enhance the need for future research.

Acknowledgements

The first author gratefully appreciates the School of Engineering and Birmingham Centre for Railway Research and Education of his PhD scholarship. The authors are sincerely grateful to European Commission for the financial sponsorship of the H2020-RISE Project No. 691135 "RISEN: Rail Infrastructure Systems Engineering Network", which enables a global research network that tackles the grand challenge in railway infrastructure resilience (Kaewunruen *et al*. 2016) and advanced sensing in extreme environments (www.risen2rail.eu).

References

Abbas, A., Masad, E., Papagiannakis, T. and Harman, T. (2007), "Micromechanical modelling of the viscoelastic behavior of asphalt mixtures using the discrete-element method", *Int. J. Geomechanics*, **7**(2), 131-139.

Abdelkrim, M., Bonnet, G. and de Buhan, P. (2003), "A computational procedure for predicting the long term residual settlement of a platform induced by replaced traffic loading", *Comput. Geotech.*, **30**(6), 463-476.

Aikawa, A. (2017), "Impact-loading-test regarding ballast subsidence countermeasurs using high-damping under sleeper pads and high-strength artificial ballast cubes", *Proceedings of the 14th International conference & Exhibition of Railway Engineering*, Edinburgh, UK.

Alva-Hurtado, J.E. and Selig, E.T. (1981), "Permanent strain behavior of railroad ballast", *Proceeding of the International Conference on Soil Mechanics and Foundation Engineering*, **1**, 543-546.

Barr, A.H. (1981), "Superquadrics and Angle-Preserving Transformations", *IEEE Comput. Graph. Appl.*, 1(1), 11-23.

Chazallon, C., Koval, G. and Mouhoubi, S. (2012), "A two-mechanism elastoplastic model for shakedown of unbound granular materials and DEM simulations", *Int. J. Numer. Anal. Method. Geomech.*, **36**(17), 1847-1868.

Chen, C., McDowell, G.R. and Thom, N.H. (2014) "Investigating geogrid-reinforced ballast: experimental pull-out tests and discrete element modeling", *Soils Found*, **54**(1), 1-11.

Chung, Y.C. and Ooi, J.Y. (2008), "A study of influence of gravity on bulk behaviour of particulate solid", *Particuology*, **6**, 467-474.

Cundall, P.A. (1971), "A Computer Model for Simulating Progressive, Large Scale Movements in Blocky Rock Systems", *International Symposium on Rock Fracture, I.S.R.M.*, Nancy, France.

Cundall, P.A. and Strack, O.D.L. (1979), "A discrete numerical model for granular assemblies", *Geotechnique*, **29**(1), 47-65.

Cundall, P.A. (1988), "Formulation of a Three-Dimensional Distinct Element Model -- Part I. A Scheme to Detect and Represent Contacts in a system Composed of Many Polyhedral Blocks", *Int. J. Rock Mech., Min. Sci. Geomech. Abstr.*, **25**(3), 107-116.

Cundall, P.A. and Hart, R.D. (1992), "Numerical modeling of discontinua", *Engr. Comp*., **9**(2), 101-103.

Di Renzo, A. and Di Maio, F. P. (2005), "An improved integral non-linear model for the contact of particles in distinct element simulations", *Chem. Eng. Sci.*, **60**(5), 1303-1312.

Eliáš, J. (2013), "DEM simulation of railway ballast using polyhedral elemental shapes", *Proceedings of the 2nd international conference on particle-based methods - fundamentals and applications*, Stuttgart, Germany.

Esveld, C., (2001), *Modern Railway Track*, second ed., MRT-Productions, Netherlands.

Ferellec J.F. and McDowell, G.R. (2010) "A method to model realistic particle shape and inertia in DEM", *Granul Matter*, **12**(5), 459-467.

Gallego, I., Muñoz, J., Rivas, A. and Sanchez-Cambronero, S. (2011), "Vertical track stiffness as a new parameter involved in designing high-speed railway infrastructure", *J. Transport. Eng.*, **137**(12), 971-979.

Gallego, I., Pita, A.L., Chaves, E.W.V. and Álvarez, A.M.R. (2011), "Design of embankment–structure transitions for railway infrastructure", *Proc. ICE-Transport*, **165**(1), 27-37.

Gallego, I., Rivas, A. and Sánchez-Cambronero, S. (2012), "Criteria for Improving the Embankment-Structure Transition Design in Railway Lines", INTECH Open Access Publisher, Croatia.

Garcia, X., Xiang, J., Latham, J.P. and Harrison J.P. (2009) "A clustered overlapping sphere algorithm to represent real particles in discrete element modeling", *Géotechnique*, **59**(9), 779-784.

Hertz, H. (1895), "Ueber die Beruehrung Elastischer Koerper (On Contact between Elastic Bodies)", *in Gesammelte Werke (Collected Works)*, Leipzig, Germany.

Hess, W. and Schonert, K. (1981), "Brittle-plastic transition in small particles", *Proceedings of the Powtech Conference on Particle Technology*, Birmingham, UK.

Hohner, D., Wirtz, S. and Scherer, V. (2013), "Experimental and numerical investigation on the influence of

particle shape and shape approximation on hopper discharge using the discrete element method", *Powder Technol.*, **235**, 614-627.
Indraratna, B., Wijewardena, S. and Balasubramaniam, A.S. (1993), "Large scale triaxial testing of a greywacke rockfill", *Ge´otechnique*, **43**(1) 37-51.
Indraratna, B., Ionescu, D. and Christie, H.D. (1998), "Shear behaviour of railway ballast based on large-scale triaxial tests", *J. Geotech. Geoenviron. Eng. - ASCE*, **124**(5), 439-449.
Indraratna, B., Ionescu, D. and Christie, H.D. (1998), "Shear behaviour of railway ballast based on large-scale triaxial tests", *J. Geotech. Geoenviron. Eng. - ASCE*, **124**(5), 439-449.
Indraratna, B. and Salim, W. (2002). "Modelling of particle breakage of coarse aggregates incorporating strength and dilatancy", *Proc. Instn Civ. Engrs Geotech. Eng.*, **155**(4) 243-252.
Indraratna, B., Lackenby, J. and Christie, H.D. (2005), "Effect of confining pressure on the degradation of ballast under cyclic loading", *Ge´otechnique*, **55**(4) 325-328.
Indraratna, B., Salim, W. and Rujikiatkamjorn, C. (2011), Adavanced Rail Geotechnology-Ballasted Track , Taylor & Francis Group, London, UK.
Indraratna, B., Nimbalkar, S. and Rujikiatkamjorn, C. (2011), "Stabilisation of ballast and subgrade with geosynthetic grids and drains for rail infrastructure", *Proceedings of the International Conference on Advances in Geotechnical Engineering*, Perth, Australia.
Indraratna, B., Ngo, N., Rujikiatkamjorn, C. and Vinod, J.S. (2014), "Behavior of fresh and fouled railway ballast subjected to direct shear testing: discrete element simulation", *Int. J. Geomechanics*, **14**(1), 34-44.
Irazabel, J., Salazar, F. and Onate, E. (2017), "Numerical modelling of granular materials with spherical discrete particles and the bounded rolling friction model. Application to railway ballast", *Comput. Geotechnics*, **85,** 220-229.
Itasca (2003), Particle Flow Code in Two Dimensions, Itasca Consulting Group, Inc., Minnesota. USA.
Jung, S.D., Kim, J.S., Park, J.W., Won, J.H. and Kim, M.K. (2013), "Distinct element method analysis of a retaining wall using a steel frame and fill materials", *Multimedia Tools Appl.*, **74**(20), 9017-9029.
Kaewunruen, S. (2014), "Monitoring in-service performance of fibre-reinforced foamed urethane material as timber-replacement sleepers/bearers in railway urban turnout systems", *Struct. Monit. Maint.*, **1**(1), 131-157 (invited).
Kaewunruen, S. and Kimani, S.K. (2017), "Damped frequencies of pre-cast modular steel-concrete composites railway track slabs", *Steel Compos. Struct*., in press.
Kaewunruen, S. and Mirza, O. (2017), "Hybrid discrete element – finite element simulation for railway bridge-track interaction", *Proceedings of the 3rd International Conference on Innovative Materials, Structures and Technologies*, Riga Technical University, Riga, Latvia, 27-29 September 2017.
Kaewunruen, S. and Remennikov, A.M. (2010), "Dynamic properties of railway track and its components: Recent findings and future research direction", *Insight: Non-Destructive Testing and Condition Monitoring*, **52**(1), 20-22.
Kaewunruen, S., Remennikov, A.M. and Murray, M.H. (2014), "Introducing limit states design concept to concrete sleepers: an Australian experience", *Frontiers in Mat*., **1**(8), 1-3.
Kaewunruen, S., Sussman, J.M. and Matsumoto, A. (2016), "Grand challenges in transportation and transit systems", *Front. Built Environ*., 2:4. doi: 10.3389/fbuil.2016.00004
Kimani, S.K. and Kaewunruen, S. (2017), "Free vibrations of pre-cast modular steel-concrete composites railway track slabs", *Steel Compos. Struct*., *in press.*
Kumara, J.J. and Hayano, K. (2016), "Importance of particle shape on stress-strain behaviour of crushed stone-sand mixtures", *Geomech. Eng.*, **10**(4), 455-470.
Lane, J.E., Metzger, P.T. and Wilkinson, R.A. (2010), A Review of Discrete Element Method (DEM) Particle Shapes and Size Distributions for Lunar Soil, National Aeronautics and Space Administration, Cleveland, Ohio, USA.
Lim, W. L. (2004), "Mechanics of railway ballast behaviour", Ph.D. Dissertation, University of Nottingham, UK.
Lim, W.L., McDowell, G.R. and Collop, A.C. (2004), "The application of Weibull statistics to the strength of railway ballast", *Granular Matter*, **6**, 229-237.

Lim, W. and McDowell, G. (2005), "Discrete element modelling of railway ballast", *Granular Matter*, **7**, 19-29.
Lobo-Guerrero, S., Vallejo, L.E. and Vesga, L.F. (2006), "Visualization of Crushing Evolution in Granular Materials under Compression Using DEM", *Int. J. Geomech.*, **6**(3), 195-200
Lobo-Guerrero, S. and Vallejo, L.E. (2006), "Discrete element method analysis of railtrack ballast degradation during cyclic loading", *Granular Matter*, **8**(3-4), 195-204.
Mahmouda, E., Papagiannakisb, A.T. and Renteriaa, D. (2016), "Discrete element analysis of railway ballast under cycling loading", *Procedia Eng*., **143**, 1068-1076.
Marsal, R.J. (1973), "Mechanical properties of rockfill", John Wiley & Sons, New York, USA
Matsushima, T., Katagiri, J., Uesugi, K., Tsuchiyama, A. and Nakano, T. (2009) "3D shape characterization and image-based DEM simulation of the lunar soil simulant FJS-1", *J Aerospace Eng*., **22**(1), 15-23.
Mindlin, R.D. and Deresiewicz, H. (1953), "Elastic spheres in contact under varying oblique force", *J. Appl. Mech*, **20**, 327-344.
Nezami, E.G., Hashash, Y.M.A., Zhao, D. and Ghaboussi, J. (2004), "A fast contact detection algorithm for 3-D discrete element method", *Comput. Geotech.*, **31**, 575-587.
Nezami, E.G., Hashash, Y.M.A., Zhao, D. and Ghaboussi, J. (2006), "Shortest link method for contact detection in discrete element method", *Int. J. Numer. Anal. Meth. Geomech.*, **30**, 783-801.
Ngo, N.T., Indraratna, B. and Rujikiatkamjorn, C. (2014) "DEM simulation of the behaviour of geogrid stabilised ballast fouled with coal", *Comput Geotech.*, **55**, 224-231.
Nguyen, V., Duhamel, D. and Nedjar, B. (2003), "A continuum model for granular materials taking into account the no-tension effect", *Mech. Mater.*, **35**, 955-967.
Ouhbi N., Voivret, C., Perrin, G. and Roux J. (2016), "Railway ballast: Grain shape characterization to study its influence on the mechanical behaviour", *Procedia Eng*., **143**, 1120-1127.
Podlozhnyuk, A. and Kloss, C. (2015), "A contact detection method between two convex super-quadric particles based on an interior point algorithm in the discrete element method", *Proceedings of the IV International Conference on Particle-Based Methods*, Barcelona, Spain.
Prescott, D. and Andrews, J. (2013), "A track ballast maintenance and inspection model for a rail network", *Proc IMechE Part O: J Risk and Reliability*, **227**(3), 251-266
Ricci, L., Nguyen, V., Sab, K., Duhamel, D. and Schmitt, L. (2005), "Dynamic behaviour of ballasted railway tracks: A discrete/continuous approach", *Comput. Struct.*, **83**, 2282-2292.
Remennikov, A.M. and Kaewunruen, S. (2008), "A review of loading conditions for railway track structures due to train and track vertical interaction", *Struct. Control. Health Monit*., **15**(2), 207-234.
Remennikov, A.M. and Kaewunruen, S. (2014), "Experimental load rating of aged railway concrete sleepers", *Eng. Struct*., **76**(10), 147-162.
Sasaoka, C.D. and Davis, D. (2005), "Implementing track transition solutions for heavy axle load service", *Proceedings of the AREMA 2005 Annual Conference*, Chicago, IL,
Sato, Y. (1995), "Japanese studies on deterioration of ballasted track", *Vehicle Syst. Dynam*., **24**(1), 197-208.
Selig, E.T. and Alva-Hurtado, J.E. (1982), "Predicting effects of repeated wheel loading on track settlement", *Proceedings of the 2nd Int. Heavy Haul Railway Conf*., Colorado Springs, USA.
Selig, E.T. and Waters, J.M. (1994), Track Geotechnology and Substructure Management, Thomas Telford Publishing, UK.
Setsobhonkul, S., Kaewunruen, S. and Sussman, J.M. (2017), "Lifecycle assessments of railway bridge transitions exposed to extreme climate events", *Front. Built Environ*., 3:35. doi: 10.3389/fbuil.2017.00035
Sharp, R.W. and Booker, J.R. (1984), "Shakedown of pavement under moving surface loads", *J. Transportation Eng*., **110**(1), 1-14.
Shenton, M. (1985), "Ballast deformation and track deterioration", *Track technology*, 253-265.
Smilauer, V., Catalano, E., Chareyre, B., Dorofenko, S., Duriez, J., Gladky, Kozˇicki, J., Modenese, C., Scholt`es, L., Sibille, L., Str´ansk´y, J. and Thoeni, K. (2010), Yade Documentation (1st Ed.), The Yade Project. http://yade-dem.org/doc/.
Suiker, A.S.J. and Borst, R. (2003), "A numerical model for the cyclic deterioration of railway tracks", *Int. J. Numer. Meth. Eng.*, **57**(4), 441-470.

Standards Australia (1996), Aggregates and rock for engineering purposes. Standards Association of Australia; Australia.

Thakur, P.K., Indraratna, B. and Vinod, J.S. (2009), "DEM simulation of effect of confining pressure on ballast behaviour", *Proceedings of the 17th International Conference on Soil Mechanics and Geotechnical Engineering*.

Thakur, P.K., Vinod, J.S. and Indraratna, B. (2010), "Effect of particle breakage on cyclic densification of ballast: a DEM approach", *Proceedings of the 9th World Congress on Computational Mechanics and 4th Asian Pacific Congress on Computational Mechanics*, 19-23 Jul, 2010, Sydney, Australia, IOP Conference Series: Materials Science and Engineering, **10**(1), 1-7.

Tutumluer, E. (1995), "Prediction Behavior of Flexible Pavements with Granular Bases", Ph.D. Dissertation, Georgia Institute of Technology, Atlanta, USA.

Tutumluer, E., Huang H., Hashash, Y.M.A. and Ghaboussi, J. (2006), "Aggregate Shape Effects on Ballast Tamping and Railroad Track Lateral Stability", *Proceedings of the AREMA Conference*, Louisville, KY, USA.

Tutumluer, E., Huang, H., Hashash, Y.M.A. and Ghaboussi, J. (2007), "Discrete element modeling of railroad ballast settlement", *Proceedings of the AREMA Conference*, Chicago, IL, USA

Tutumluer, E., Huang, H., Hashash, Y.M.A. and Ghaboussi, J. (2008), "Contact stiffness affecting discrete element modeling of unbound aggregate granular assemblies", *Proceedings of the 7th UNBAR Conference*, Nottingham, UK.

Wang, Z., Ruiken, A., Jacobs, F. and Ziegler, M. (2014), "A new suggestion for determining 2D porosities in DEM", *Geomech. Eng.*, **7**(6), 665-678.

Xu, W.J., Li, C.Q. and Zhang, H.Y. (2015), "DEM analyses of the mechanical behavior of soil and soil-rock mixture via the 3D direct shear test", *Geomech. Eng.*, **9**(6), 815-827.

Yan, Y., Zhao, J. and Ji, S. (2015), "Discrete element analysis of breakage of irregularly shaped railway ballast", *Geomech. Geoeng.*, **10**(1), 1-9.

Zhou, L., Chu, X., Zhang, X. and Xu, Y. (2016) "Numerical investigations on breakage behaviour of granular materials under triaxial stresses", *Geomech. Eng.*, **11**(5), 639-655.

JK